

Rapid Oscillations in Cataclysmic Variables. XIII. WZ Sagittae Revisited

JOSEPH PATTERSON,^{1,2} HAYLEY RICHMAN,³ AND JONATHAN KEMP¹

Department of Astronomy, Columbia University, 550 West 120th Street, New York, NY 10027;
jop@astro.columbia.edu, jonathan@astro.columbia.edu

AND

KOJI MUKAI

Laboratory for High Energy Astrophysics, Goddard Space Flight Center, National Aeronautics and Space Administration,
MS 660.2, Greenbelt, MD 20771; mukai@lheavx.gsfc.nasa.gov

Received 1997 September 18; accepted 1998 January 16

ABSTRACT. We report new observations of the dwarf nova WZ Sagittae, showing the return of the 27.87 s oscillation in 1995/1996 high-speed optical light curves. As was true in 1978, the main peak of the power spectrum generally occurred at 27.87 or 28.96 s, with the signals sometimes simultaneously present. Weak transient signals were also seen at 28.20 and 29.69 s. An *ASCA* X-ray observation showed a significant peak at 27.86 ± 0.01 s in the 2–6 keV band, which appeared to establish the star’s membership as a “DQ Herculis star,” in which accretion onto the white dwarf is channeled by a strong magnetic field. The X-ray period is most likely the true white dwarf spin period. However, we certainly do not understand the distribution of power among these various signals of slightly different period. This puzzling multiperiodic structure remains an impediment to full acceptance of WZ Sge as a DQ Her star. The star’s soft X-ray orbital light curve shows a strong but transient energy-dependent dip around orbital phase 0.7, which is probably due to absorption by an extended gas cloud in which the mass-transfer stream strikes the disk.

1. INTRODUCTION

Throughout the 1960s and 1970s one of the most thoroughly studied cataclysmic variables was the dwarf nova WZ Sagittae. The basic parameters of the binary star model were found by Krzeminiński & Kraft (1964) and Krzeminiński & Smak (1971). A very low mass secondary star orbits a white dwarf with a period of 81.6 minutes. Most of the visual light probably originates from the white dwarf, although the accretion disk/stream also contributes a weak continuum and strong hydrogen emission lines. The orbital period itself is manifest primarily in a sharp but shallow eclipse of a small object, which is usually assumed to be the mass-transfer bright spot. A recent summary and study of the star’s properties is given by Smak (1993).

A curious feature appeared with the discovery of coherent 28 s oscillations in the quiescent light curve (Robinson, Nather, & Patterson 1978; hereafter RNP). RNP interpreted this as signifying nonradial pulsation of the white dwarf, mainly be-

cause they detected two noncommensurate signals simultaneously present (at 27.87 and 28.97 s). Patterson (1980; hereafter P80) studied a large set of 1976–1978 data and found that the 27.87 s signal was basically phase stable from night to night. He interpreted the data in terms of magnetically channeled accretion onto the white dwarf and attributed the “satellite periods” (the 28.97 s signal and several others in the low-frequency wing of the principal 27.87 s signal) to reprocessing in structures moving prograde in the accretion disk.

Magnetically channeled accretion flow onto a rapidly rotating white dwarf should produce X-ray pulses at the rotation period. We have been searching for these and have been seeking to study further the optical oscillations for nearly 20 years. But when the star suffered a dwarf nova outburst in 1978, the oscillation disappeared (Patterson et al. 1981). Posteruption optical photometry showed weak, transient signals at several of the satellite periods (Middleditch & Nelson 1980; Skidmore et al. 1997) but did not show the principal signal seen before eruption. X-ray observations have given only null results for pulsations (Eracleous, Patterson, & Halpern 1991b).

In 1995, our patience was rewarded when the principal 27.87 s optical signal returned. Soon thereafter we followed up with an *ASCA* X-ray observation, which appeared to show X-ray pulses. In this paper we describe these results, sort among the various and often confusing lines of evidence, and interpret

¹ Visiting Astronomer, Cerro Tololo Inter-American Observatory, National Optical Astronomy Observatories, which is operated by the Association of Universities for Research in Astronomy, Inc. (AURA), under cooperative agreement with the National Science Foundation.

² Visiting Astronomer, Kitt Peak National Observatory, National Optical Astronomy Observatories.

³ Current address: 400 East 84th Street, 34B, New York, NY 10028; hayley.richman@gs.com.

TABLE 1
LOG OF OPTICAL OBSERVATIONS

UT Date	Telescope	UT Start	Duration (hr)	Δt (s)	Points
1982 Nov 13	KPNO 0.9 m	1:42:29	0.50	10.004	180
1983 Oct 10	KPNO 0.9 m	2:45:56	1.01	5.004	721
1985 Nov 17	KPNO 0.9 m	2:33:07	1.70	5.004	1224
1988 May 20	KPNO 0.9 m	9:06:08	1.90	5.004	1354
1988 May 22	KPNO 0.9 m	9:12:43	1.81	5.004	1298
1990 Jul 23	Lick 1 m	6:41:05	2.00	9.000	800
1995 Jun 29	CTIO 1 m	3:49:58	5.12	5.808	3012
1995 Jun 30	CTIO 1 m	3:42:56.2	2.01	5.801	1019
1995 Jul 2	CTIO 1 m	4:28:39	3.97	5.804	1126
1995 Jul 3	CTIO 1 m	3:48:29	4.85	5.684	2874
1995 Jul 6	CTIO 1 m	3:34:18.8	4.89	2.000	8479
1995 Jul 7	CTIO 1 m	3:25:59.6	1.94	2.000	3503
1995 Jul 8	CTIO 1 m	3:23:38.4	3.30	2.000	5616
1996 Jul 11	CTIO 1 m	5:33:20.7	2.53	5.000	1707
1996 Jul 12	CTIO 1 m	3:11:51	4.81	5.000	3343
1996 Jul 14	CTIO 1 m	3:03:32.6	4.84	5.000	3486
1996 Jul 17	CTIO 1 m	2:57:37.4	5.0	5.000	3206
1996 Jul 18	CTIO 1 m	3:15:01.0	4.70	5.000	3256
1996 Jul 19	CTIO 1 m	4:08:28.0	3.0	5.000	2180
1996 Jul 21	CTIO 1 m	3:17:36.0	3.67	5.000	2607
1996 Jul 23	CTIO 1 m	1:54:53.8	4.84	5.000	3486
1996 Aug 8	CTIO 1 m	1:12:21.8	4.98	5.000	3583
1996 Aug 11	CTIO 1 m	0:38:03.6	4.80	3.000	5756
1996 Aug 12	CTIO 1 m	1:13:47.6	4.79	3.000	5437
1996 Aug 15	CTIO 1 m	1:44:08.7	4.17	3.000	4840
1996 Aug 16	CTIO 1 m	1:38:08.4	4.33	3.000	5002
1996 Aug 17	CTIO 1 m	1:27:15.3	4.29	3.000	5115

WZ Sge as containing an accreting magnetic white dwarf. It is far from a typical member of this class, and we interpret its deviations from the norm as arising from the smallness of its magnetic field and accretion rate and from the speed of its rotation.

2. OPTICAL OBSERVATIONS

2.1. Data Acquisition, Reduction, and Light Curves

Our optical observations consist of high-speed photometry obtained with various telescopes and photometers since 1979. Mostly we used photomultiplier tubes with natural cutoffs redward of $\sim 5800 \text{ \AA}$ or copper sulfate filters to achieve the same results. Effectively the bandpass can be considered “broad B .” A summary is given in the optical observing log presented as Table 1.

WZ Sge has an optical companion $8''$ to the west, a nuisance for aperture photometers. On nights of good seeing, we used a small focal-plane aperture and guided carefully to keep the companion away; on poor nights, we included the companion by using a bigger aperture and then in data analysis subtracted a constant signal representing the companion star’s unwanted light. We reduced the data by subtracting the sky contribution and using a mean extinction coefficient to convert to counts per second above the atmosphere.

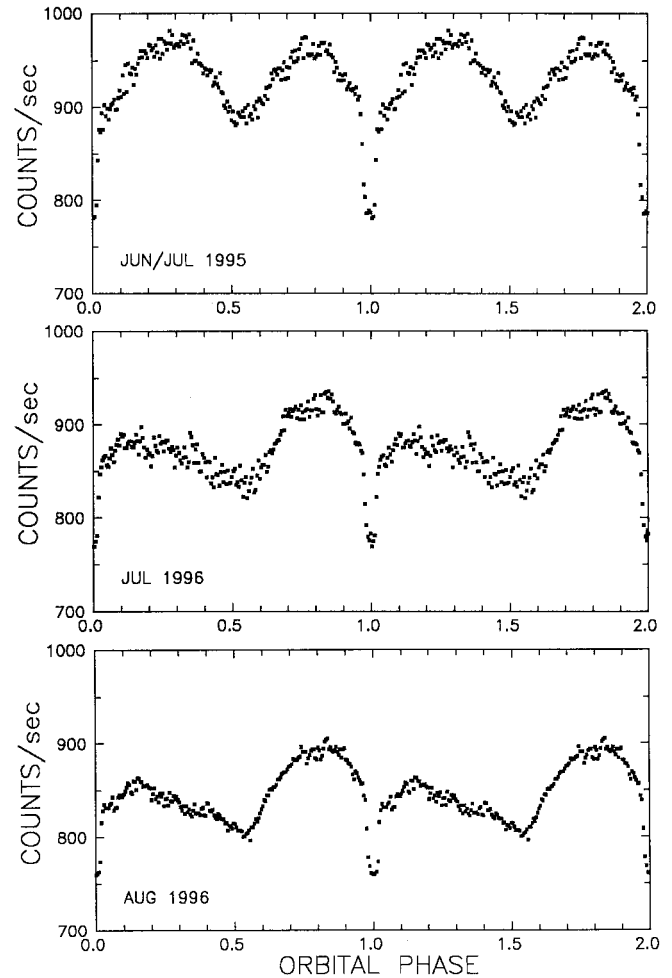


FIG. 1.—Average orbital light curves in blue light (copper sulfate filter) at three different epochs, binned with 24.49 s per point. A value of 1000 counts s^{-1} corresponds approximately to $B = 15.37$ mag in 1996; the 1995 calibration is not securely known.

The nightly light curves greatly resembled those presented by RNP and P80: a sharp eclipse defining phase zero and a usually double-humped photometric wave. As remarked by RNP and Krzemiński & Kraft (1964), the hump after eclipse is often broken up by apparent absorption events, which renders it smaller and less distinct in the mean light curve. This is shown in Figure 1, where we segregate the data into three bins (1995 June/July, 1996 July, and 1996 August), suggested by the clustering of the data and the properties of the rapid oscillation.

2.2. Periodicity Search

We searched all light curves for the presence of periodic signals by calculating the power spectrum from the discrete Fourier transform. At low frequencies the results were uninteresting: peaks at ν_{orb} and its low harmonics (down to the

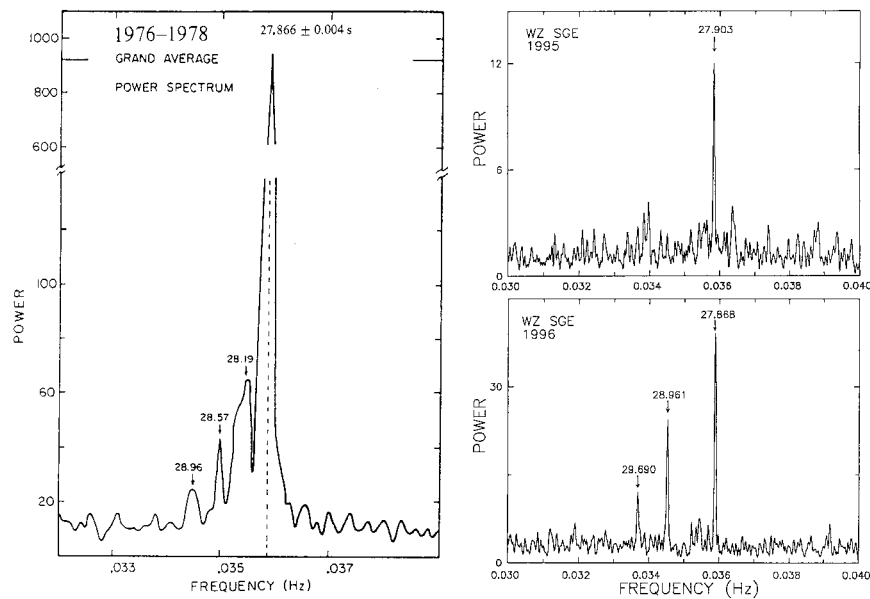


FIG. 2.—*Left*: average power spectrum during 1976–1978, showing a strong signal at 27.866 s and weak low-frequency sidebands. *Upper right*: the average during 1995; *lower right*: the average during 1996. In 1995/1996 the average semiamplitude of the principal oscillation was 0.003 mag (with considerable variation), about the same as 1976–1978. Signals are marked with their periods in seconds.

eighth). The average high-frequency power spectrum over 30 nights during 1976–1978 is shown in the left-hand frame of Figure 2. Basically there was a strong signal at 27.866 s (averaging 0.004 mag semiamplitude but varying in the range $0.001\text{--}0.010 \text{ mag}$), with weak low-frequency sidebands at 28.96, 28.52, and 28.19 s. The weakness of the sidebands made it possible to count cycles in the main signal from night to night, and P80 found that signal to be nearly stable at 27.8684 s during 1978. During the coverage of the 1978 December outburst, no signals were found to a semiamplitude upper limit of 0.0007 mag .

Sporadic coverage during 1979–1991 showed weak signals (about 0.002 mag semiamplitude when seen, but often ebbing below the typical detection threshold of 0.001 mag) in the period range $28.2\text{--}29.7 \text{ s}$. The signal at 28.96 s, familiar from preoutburst photometry, was frequently seen, as reported also by Middleditch & Nelson (1982) and Skidmore et al. (1997). The dominant preoutburst signal at 27.87 s never appeared.

The light curves of 1995 and 1996 showed the return of the principal oscillation. The rightmost panels of Figure 2 show the mean nightly power spectra from these two observing seasons. The strongest signal occurred at $\sim 27.88 \text{ s}$, with smaller peaks at 28.96 and 29.69 s, and probably also a little bump in the immediate low-frequency wing of the main signal (the highest peak occurring at 28.22 s). Inspection of the individual nights showed that these signals seldom coexisted and certainly not at amplitudes consistent with the mean results of Figure 2. Most nights were dominated by either 27.87 or 28.96 s at semiamplitudes around 0.004 mag . Some episodes did seem

to occur when they were simultaneously present, however; it was difficult to be sure because the oscillation requires an observation of several hours to detect securely, yet amplitude changes seem to occur on that timescale or even faster.

2.3. The 27.87 Second Oscillation

We studied the short-period oscillation most thoroughly because a preoutburst period of high precision is known. The mean nightly period was $27.903 \pm 0.015 \text{ s}$ in 1995 and $27.868 \pm 0.009 \text{ s}$ in 1996 July (there was no detection in 1996 August). Neither of these periods was quite precise enough to solve the problem of cycle count across a 1 day gap, so we do not confidently know the precise period in either year. Do these observations in successive years sample the same periodic process? The possible (2σ) period shift in 1995/1996 is worrisome. But no such shift was ever found in the 1970s photometry, so we take these period estimates at face value, assume that no large period change occurred during 1995/1996, and express the best estimate as $27.877 \pm 0.010 \text{ s}$.

P80 found a characteristic wander in the nightly pulse timings of $\sim 3 \text{ s}$, and we found a similar wander. This made precise period-finding difficult. The 1995 data gave no really acceptable candidate period of high precision, but the 1996 data gave candidates of 27.8666 and 27.8757 (± 0.0001) s.

It was curious that the 1996 August data showed no detection of the 27.87 s signal (to a limit of 0.001 mag in the average power spectrum), despite a large amount of good data. In fact 1996 July and 1996 August are similar in quantity and quality

TABLE 2
TIMINGS OF MIDECLIPSE

HJD (2,400,000+)	HJD (2,400,000+)	HJD (2,400,000+)
45,286.5831	50,281.6327	50,307.5956
49,898.7064	50,281.6895	50,307.6517
49,904.6585	50,281.7464	50,307.7091
49,904.7153	50,281.8031	50,310.6002
49,904.7718	50,282.7100	50,310.7137
49,904.8287	50,282.7666	50,311.6205
49,905.6789	50,282.8232	50,311.6771
49,906.6994	50,283.7304	50,311.7340
49,906.7559	50,283.7866	50,312.5842
50,275.7935	50,303.5709	50,312.6407
50,276.7575	50,306.5756	50,312.6978
50,276.8144	50,306.6886	

of data and in mean light curve (see Fig. 1), but the oscillation amplitude differed by a factor greater than 3.

2.4. The 28.96 Second Oscillation

No simple pattern was found to describe the various apparitions of power at 27.87 s versus 28.96 s. But in 1996 the longer period signal dominated on each of the five nights from July 17 to July 23. This yielded five good pulse timings, which fit fairly well a best period of 28.9593(2) s. This is too weak a foundation really to prove stability (i.e., the good fit could be due to chance), but it does suggest that the 28.96 s signal may be phase stable over an interval of ~ 1 week.

2.5. Weaker Oscillations

Figure 2 shows a marked signal at 29.69 s, which was not previously seen in WZ Sge. Unlike the two stronger signals, this one never dominated and indeed was usually hidden in the noise, only emerging in the eight night average. The little bump at 28.21 s is even weaker, but it is presumably real since it is the next highest peak in the power spectrum (with ~ 400 independent frequencies) and agrees in frequency with a signal detected clearly in the 1970s photometry and in the *Hubble Space Telescope* (*HST*) ultraviolet continuum (Welsh et al. 1997; C. A. Haswell 1997, private communication).

We do not understand the signal at 29.69 s, any more than we have ever understood the one at 28.96 s. It may be significant that $(29.69 \text{ s})^{-1}$ is within measurement error equal to $(28.96 \text{ s})^{-1} - 4(P_{\text{orb}})^{-1}$. On the other hand, it may simply reflect how many hours we spent punching calculator keys.

3. THE ORBITAL EPHEMERIS

Measurements were made of 35 eclipses and are given in Table 2. We measured the eclipse depth, width (the time interval between midingress and midegress), and time of mideclipse. The durations of ingress and egress are not well determined but are generally consistent with the results of RNP (average ingress = 100 s; average egress = 70 s). The full eclipse

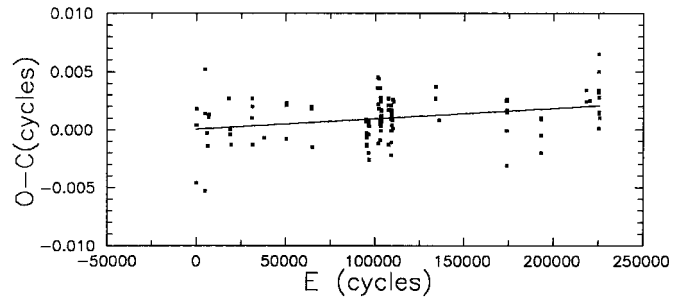


FIG. 3.— $O - C$ diagram of mideclipse timings, relative to the RNP ephemeris. The straight line is the ephemeris presented here, eq. (1).

width at half-depth was estimated by RNP as 164 ± 9 s, but it averaged 210 ± 20 s in our data.

These mideclipse timings slightly improve the optical ephemeris. We added them to those previously published and prepared Figure 3, an $O - C$ diagram showing residuals with respect to the RNP ephemeris. Here we have given one-third weight to the timings of Krzemiński & Kraft (1964), Krzemiński & Smak (1971), and the present paper but full weight to the timings of RNP, P80, and Skidmore et al. (1997) since they show a much smaller dispersion. The best representation of the eclipse times is still a constant-period ephemeris, namely the straight line shown in Figure 3:

$$\begin{aligned} \text{Mideclipse} = & \text{HJD } 2,437,547.72840 \\ & + 0.0566878460(3)E, \end{aligned}$$

with $|\dot{P}_{\text{orb}}| < 10^{-13}$. We used this ephemeris to calculate phases in this paper. Timing purists are free to add corrections for ET or TDT.

4. ROSAT X-RAY OBSERVATIONS

4.1. Observations and Light Curves

WZ Sge was observed by the *ROSAT* PSPC-B detector on 1991 April 10–11 for 18.5 ks. The data consist of 17 segments averaging ~ 18 minutes each. Source and background data were extracted from adjacent circular regions of 10 pixel ($80''$) radius. The mean count rate during the observations was 0.30 counts s^{-1} over the 0.07–2.4 keV energy range. Dependent as Table 3.

We divided the data into soft (0.07–0.4 keV, PI channels 9–41) and hard (0.4–2.4 keV, PI channels 42–256) X-rays. We formed the orbital X-ray light curve by folding the data according to the orbital ephemeris given above and found the light curves in the upper two frames of Figure 4. The one significant feature is a broad dip in soft X-rays centered on orbital phase 0.72 ± 0.03 . Because there is no corresponding decline in hard X-rays, this is almost certainly a sign of photoelectric absorption by cool gas. The ratio of soft to hard X-rays (“softness ratio”) is then a sensitive probe of that measure,

TABLE 3
LOG OF X-RAY OBSERVATIONS

UT Date	Instrument	Energy (keV)	Exposure (s)	Count Rate (s ⁻¹)
1979 Apr 30	<i>Einstein</i> IPC	0.2–4.0	3228	0.16
1980 Apr 21	<i>Einstein</i> IPC	0.2–4.0	3538	0.13
1980 May 7	<i>Einstein</i> IPC	0.2–4.0	8794	0.11
1983 Aug 4	<i>EXOSAT</i> LE/CMA	0.1–0.3	6895	0.019
	<i>EXOSAT</i> LE/CMA	0.1–0.3	9647	0.017
	<i>EXOSAT</i> LE/CMA	0.5–1.5	9444	0.006
1985 Oct 19	<i>EXOSAT</i> LE/CMA	0.1–0.3	10812	0.010
	<i>EXOSAT</i> LE/CMA	0.5–1.5	12006	0.004
1991 Apr 10	<i>ROSAT</i> PSPC	0.07–2.4	18516	0.30
1996 May 15	<i>ASCA</i>	0.5–10	39000	0.35

and we show that ratio in the lower frame of Figure 4. The prominent dip seen at orbital phase 0.7 is the “orbital dip” we shall discuss.

To ensure that this feature did not arise from just one anomalous episode, we also inspected segments of the data. Figure 5 shows the orbital light curve for three segments and demonstrates that the orbital dip is indeed a regularly repeating feature.

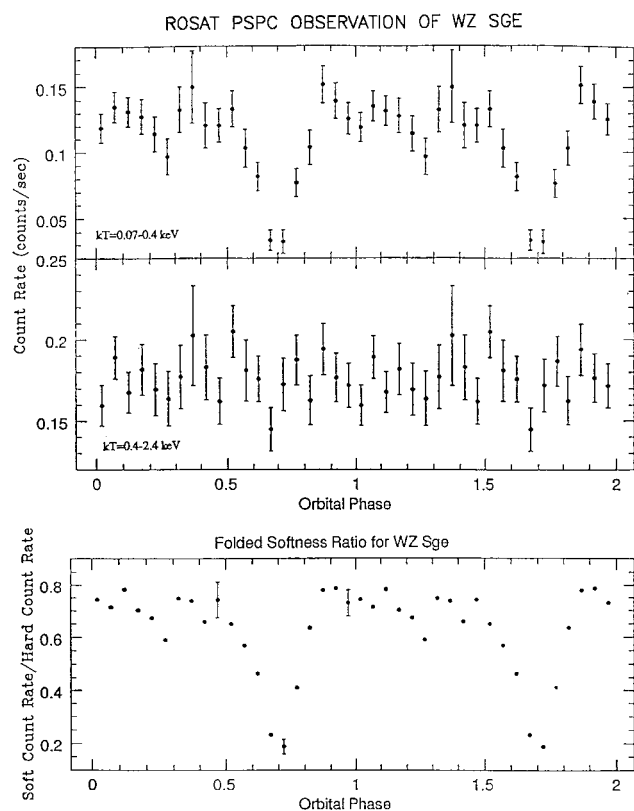


FIG. 4.—Upper two frames: orbital light curve from hard and soft X-rays in the *ROSAT* observation. Lowest frame: the ratio of soft to hard X-rays around the orbit, showing strong energy-dependent absorption near phase 0.7.

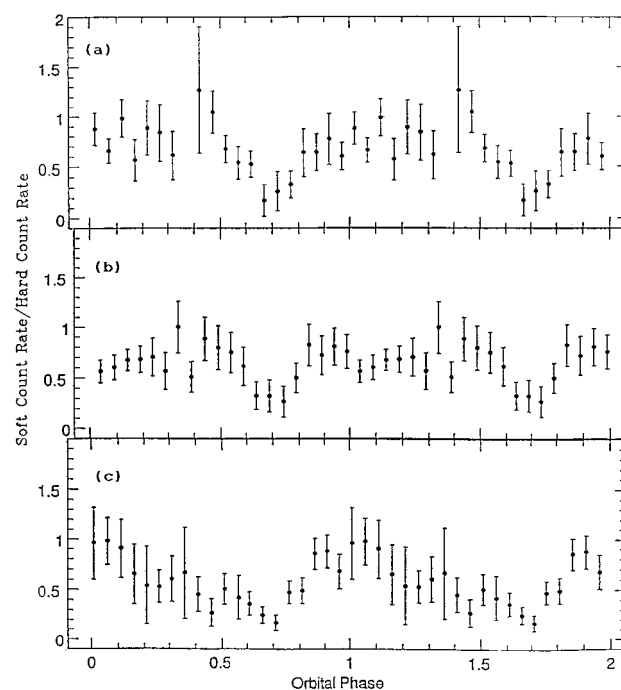


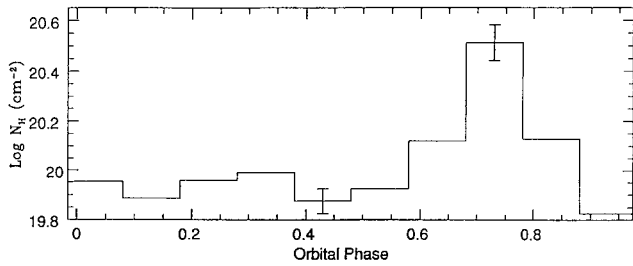
FIG. 5.—Softness ratio for three different segments of the *ROSAT* observation, showing the apparent consistency of the dip near phase 0.7.

4.2. Spectral Analysis

The background-subtracted source spectrum was binned from 256 PI channels into the PROS standard 34 channel system. Various problems are known to plague the lowest and the highest two energy channels, so we excluded them and used the remaining 31 (covering 0.07–2.4 keV) for analysis.

An acceptable fit of the data was obtained with a model of thermal bremsstrahlung emission plus absorption by an overlying layer of cool gas. With 90% confidence limits, the best fit was found with $kT = 3.0 \pm 0.9$ keV, $N_H = 8.2 \pm 2.2 \times 10^{19}$ cm⁻². By restricting the analysis to the orbital phase interval 0.9–1.2, when the X-rays appeared to be free from dips, we found $kT = 3.4 \pm 1.0$ keV, $N_H = 6.2 \pm 1.5 \times 10^{19}$ cm⁻². With these numbers we calculated an intrinsic (corrected for absorption) source flux of 1.3×10^{-12} ergs cm⁻² s⁻¹ in the 0.07–2.4 keV range.

Estimates of column density around the orbital cycle are useful in providing information about the distribution of gas in the accretion disk. To measure this, we used the Portable, Interactive, Multi-Mission Simulator (PIMMS). From the average hard X-ray count rate of 0.18 counts s⁻¹, a thermal bremsstrahlung model with the 3.4 keV out-of-dip temperature, the effective area curve of the PSPC-B detector, and a specified column density, PIMMS predicts the expected 0.07–0.4 keV count rate. Comparison with the observed count rates then yielded Figure 6, the variation of N_H with orbital phase. A large rise in column density around phase 0.75 is evident.

FIG. 6.—The variation of N_{H} with orbital phase

5. *Einstein* X-RAY OBSERVATIONS

WZ Sge was observed several times with the Imaging Proportional Counter (IPC) of the *Einstein* Observatory (Giacconi et al. 1979). These observations have been previously discussed by Eracleous et al. (1991b) and Eracleous, Halpern, & Patterson (1991a). Here we discuss only those aspects relevant to the absorption dips. We calculated a softness ratio by dividing the counts in the 0.16–0.56 keV bandpass (pulse-height channels 2–3) by the counts in the 0.56–3.5 keV bandpass (pulse-height channels 4–10), and we show its dependence on orbital phase as the points in Figure 7. We also used PIMMS to predict what this dependence should be, based on our model of the *ROSAT* result (i.e., by fixing $kT = 3.4$ keV and taking N_{H} as given in Fig. 6). The average out-of-dip IPC softness ratio should be 0.4, whereas ~ 0.2 was observed. Also, the *ROSAT* dips are essentially not seen by *Einstein*. Why is there a difference?

The absorption may have changed. Eracleous et al. (1991b) found $N_{\text{H}} = 5, 7,$ and $10 \times 10^{20} \text{ cm}^{-2}$ in the three *Einstein* observations (these three estimates agree within the errors). We repeated their analysis for the sum of the observations, finding $N_{\text{H}} = 8 \pm 4 \times 10^{20} \text{ cm}^{-2}$ (and $kT = 4 \pm 2$ keV). Thus the *Einstein* spectrum is definitely harder than that of *ROSAT*. Within our source model, we could say that the column density decreased considerably by 1991, the time of the *ROSAT* observation (the *Einstein* data were obtained soon after the 1978 dwarf nova eruption). Of course whether this is really true is impossible to know without developing X-ray source models more realistic than ours (a single-temperature source fully covered by cold absorbers).

6. *EXOSAT* X-RAY OBSERVATIONS

Five observations of WZ Sge were made with the channel electron multiplier array detector (CMA, 0.04–2.0 keV; de Korte et al. 1981) at the focus of the *European X-Ray Astronomy Satellite* low-energy imaging telescope (*EXOSAT*LE). Details are given in Table 3. The telescope has a field of view of 2° and an on-axis angular resolution of $24''$. Background data were taken from a large nearby source-free region. The detector has no intrinsic spectral capability; however, thin Lexan and aluminum/Parylene filters were used for broadband measurements.

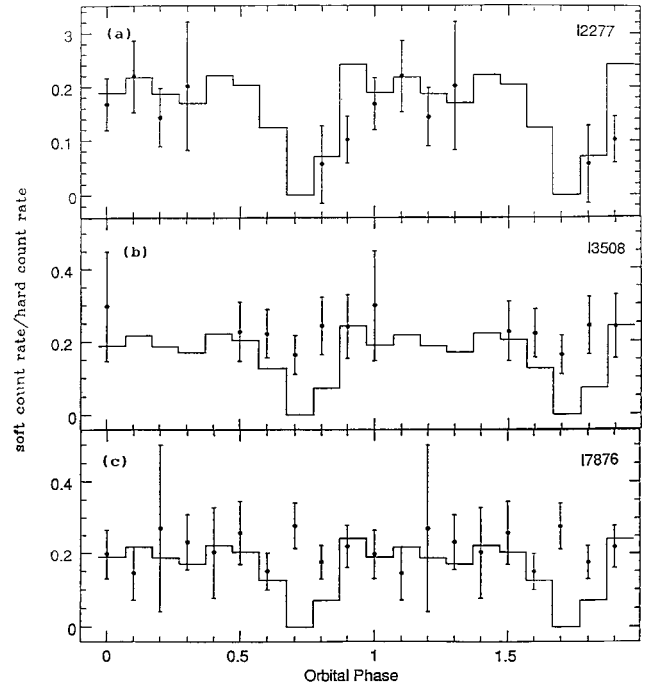


FIG. 7.—Actual and predicted softness ratios from the *Einstein* IPC observations. The data points are the ratio of the 0.16–0.56 keV to the 0.56–3.5 keV count rates in the three separate *Einstein* observations. The superposed solid line is the ratio predicted from the *ROSAT* observation but divided by 2 to overlie the data. The predicted ratio was ~ 0.4 , so the star was harder and dip-free in the *Einstein* observation.

Figure 8 shows the mean orbital light curve. The upper frame shows the average over the three Lexan (low-energy) observations, and the lower frame shows the average over the two aluminum/Parylene (higher energy) observations. As might be expected from the *ROSAT* data, a broad dip near phase 0.7 appears in the low-energy data but is invisible in the higher energy data. This was consistent with a PIMMS simulation of the *EXOSAT* light curves based on the *ROSAT* parameters.

7. *ASCA* X-RAY OBSERVATIONS AND ANALYSIS

7.1. Data Acquisition

ASCA is the fourth X-ray astronomy satellite launched and operated by ISAS, Japan, and carries four co-aligned conical-foil telescopes, two with GIS (Gas-scintillation Imaging Spectrograph) detectors and two with SIS (Solid-state Imaging Spectrograph) detectors. The *ASCA* observation of WZ Sge was carried out between 1996 May 15 455 UT and 1996 May 16 350 UT. The observation was contiguous in that no other targets were observed during this period; however, the data suffer the usual Earth occultations, SAA passages, and other instances of high background at or near the 96 minute satellite orbital period. The GISs were operated in the PH mode, while the SISs were used in 2-CCD mode, the latter limiting the time resolution to 8 s.

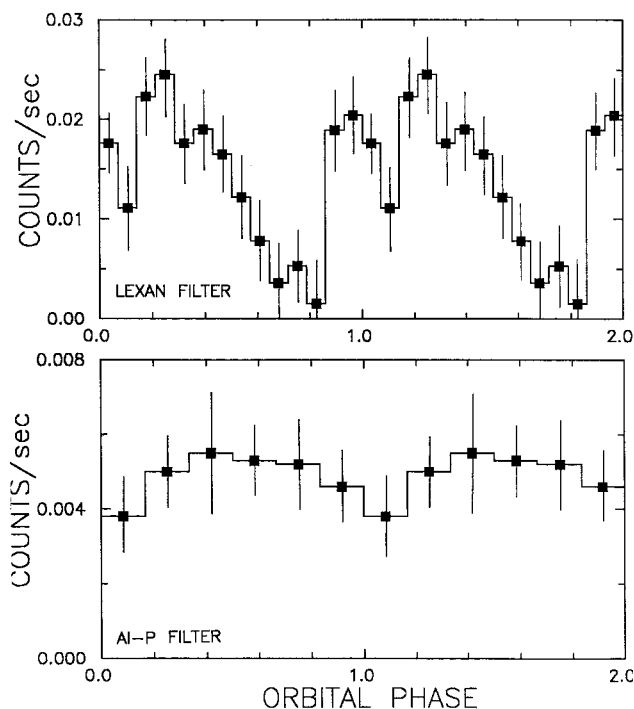


FIG. 8.—Orbital X-ray light curves in the *EXOSAT* LE. The three observations comprising the upper frame were obtained through a Lexan ($E = 0.1\text{--}0.3$ keV) filter; the two observations comprising the lower frame were obtained through an aluminum-Parylene ($E = 0.5\text{--}1.5$ keV) filter.

We removed low bit rate data, along with data taken during SAA passages, when the target was within 5° of Earth's limb and when the cutoff rigidity was below 4 GeV per count. We also eliminated the first 20 minutes of data, which were taken while the spacecraft attitude had not settled down to the final orientation. In addition, GIS data were restricted to the standard high-voltage setting; the on-board monitor L1 was used to exclude other intervals when GIS data were not being taken. Rise times of the events were used to eliminate most particle background events. SIS data were similarly screened, with the following SIS specific selection. Data taken within 10° of the bright-Earth limb were rejected. Data taken within 64 s of an orbital day/night transition or ingress/egress to the SAA were also rejected, as CCD dark levels change unpredictably at such transitions. Finally, PIXL monitor counts were used for SIS data to reject time intervals when SIS was not taking data or was suffering from high background rates. We have selected grade 0, 2, 3, 4, and 6 events and have removed hot and flickering pixels.

These acceptance criteria resulted in 35 ks of good SIS data and 39 ks of good GIS data. We used $\sim 3'2$ radius extraction regions for SIS and $\sim 6'$ regions for GIS. For local background subtraction, we used the entire area of the two CCD chips for SIS and the central $10'$ radius region of the GIS, both excluding the source region. At this small distance from the optical axis, vignetting is unimportant, the stray-light contribution is small,

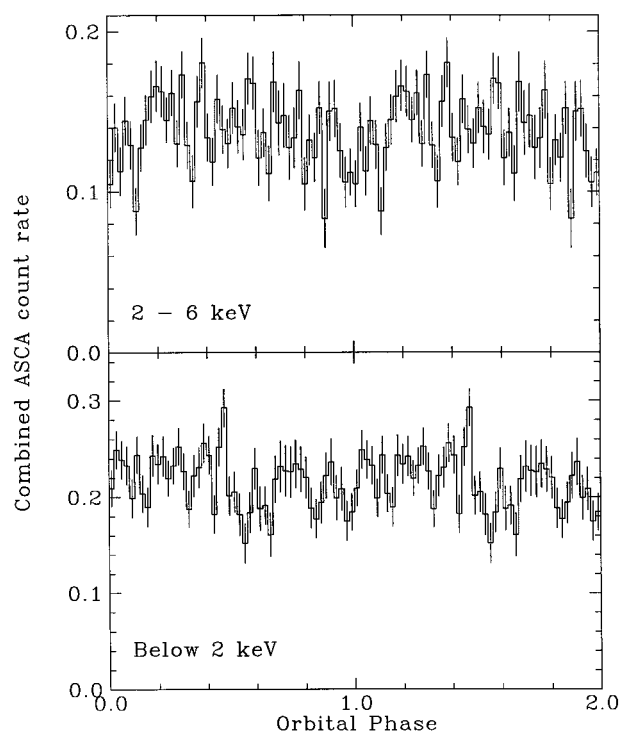


FIG. 9.—ASCA light curves, folded on P_{orb} and plotted twice, in two energy bands (*top*: 2–6 keV; *bottom*: < 2 keV). Data from all four ASCA instruments have been combined. Error bars indicate statistical 1σ errors.

and the non-X-ray background does not have a strong spatial dependence; therefore, we assumed a spatially flat background.

7.2. Light Curves

We accumulated light curves from four instruments at a time resolution of 8 s and combined them. To maximize the signal-to-noise ratio, we set an upper limit of 6 keV (0.4–6 keV for SIS, 0.7–6 keV for GIS), above which the instrumental background dominates. We also accumulated GIS light curves at a time resolution of 2 s for improved study of short periods. In addition, we divided the light curves into soft (below 2 keV) and hard (2–6 keV) bands.

7.2.1. No Orbital Modulation

In Figure 9 we show soft and hard(er) X-ray light curves, folded on the orbital ephemeris. There is little if any orbital modulation.

7.2.2. Periodicity Search

Fourier transforms of soft, hard, and combined light curves show no well-defined periodicities that are credible and significant in an unbiased search. The general noise level rises toward low frequency (“flickering”), and there are also features associated with the spacecraft orbit. In the 20–35 s range, we

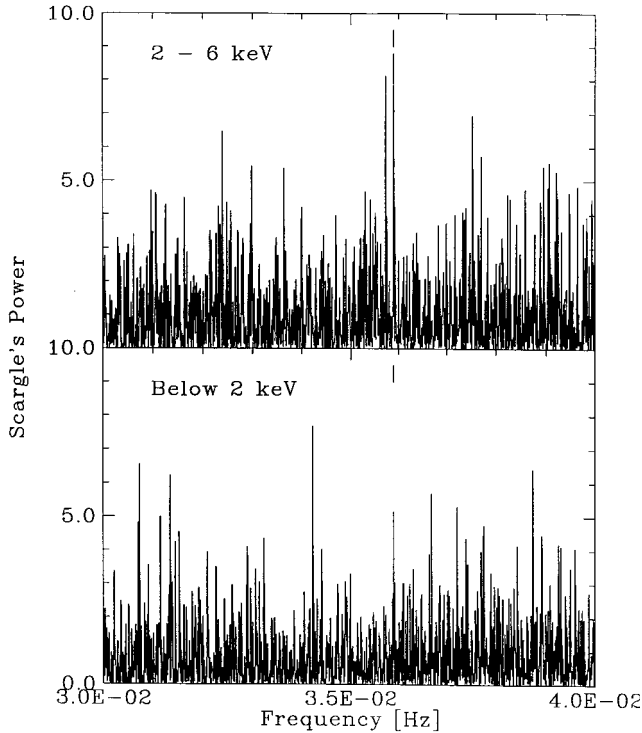


FIG. 10.—Periodograms of the ASCA hard- and soft-band light curves, as computed using Scargle's normalization, are shown in the range 30–40 mHz (25–33.3 s periods). Tick marks are placed at the period of 27.86 s, where the hard-band periodogram has the highest peak, a highly significant detection in a “period-biased” search.

estimate $\sim 7\%$ as the 90% confidence level upper limit to the semi-amplitude of any strictly periodic signal.

However, the highest power spectrum peak in this range for hard X-rays occurs at 27.86 ± 0.01 s, which is shown by the tick mark in the upper frame of Figure 10 (the immediate neighbor is an alias, created by the 94 minute spacecraft period). With ~ 400 independent frequencies in this range, the chance of a coincidental hit with a frequency known to be present in the star is only about 0.005 (see, e.g., Groth 1975). Thus we regard this as a detection of pulsed X-rays at $\sim 99.5\%$ confidence.

Interestingly, there is also a small peak at this period in the soft X-ray spectrum, shown in the lower frame of Figure 10. We were therefore puzzled as to why the more sensitive search of the combined light curve did not show evidence of pulses. We folded hard and soft X-ray light curves on the 27.86 s period and found the reason, shown in Figure 11. The two light curves are out of phase by $\sim 180^\circ$, and each has a full amplitude of ~ 0.02 counts s^{-1} , so they simply cancel each other out.

7.3. Spectroscopy

We performed simultaneous fitting of spectra obtained with the four ASCA instruments. An acceptable fit (reduced $\chi^2 =$

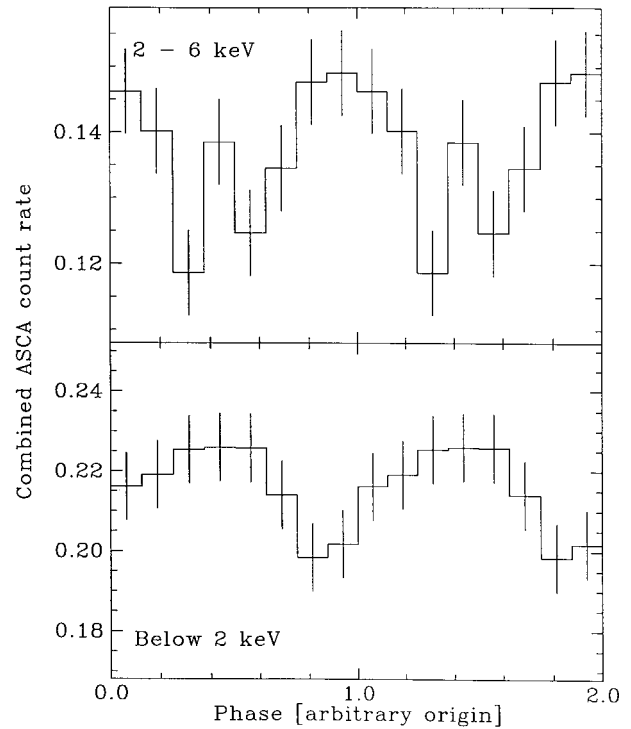


FIG. 11.—Hard and soft X-ray ASCA light curves, folded on the 27.86 s period (with an arbitrary epoch). Data are for all four instruments combined. The light curves are about a half-cycle out of phase.

1.13) was obtained with a power-law model (index 2.05, $N_H = 1.9 \times 10^{21} \text{ cm}^{-2}$). But a thermal bremsstrahlung model produced a formally better fit (reduced $\chi^2 = 1.09$) and is certainly more physically plausible. The fit is shown in Figure 12. The best-fit parameters are $kT = 4.5 \pm 0.4$ keV, $N_H = 6.5 \pm$

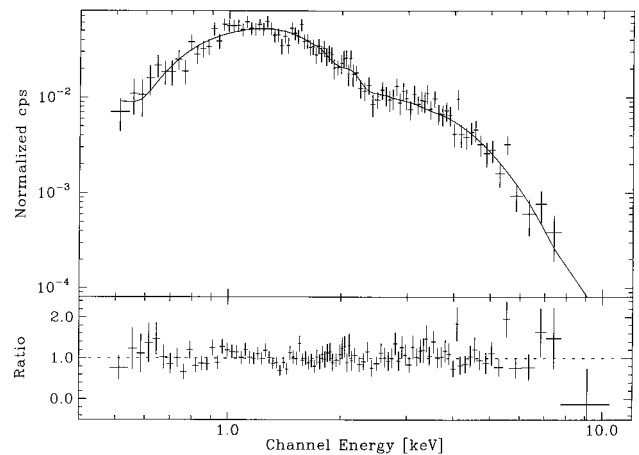


FIG. 12.—X-ray spectrum of WZ Sge, as obtained with ASCA SIS-1, is plotted with a bremsstrahlung model (see text for model parameters). We show the SIS-1 spectrum only for clarity of presentation; identical (to within statistics) spectra were obtained with the other three instruments.

$2.1 \times 10^{20} \text{ cm}^{-2}$, with a total 0.4–10 keV flux of $4.0 \times 10^{-12} \text{ ergs cm}^{-2} \text{ s}^{-1}$ uncorrected for absorption.

Although we would expect a prominent Fe K line from a plasma of this temperature, there is no obvious sign of it in the spectrum. In fact, a solar abundance Raymond-Smith model fit is much poorer (reduced $\chi^2 = 1.33$ for the best-fit temperature of 4.2 keV.) When the abundance is included in the fit (overall abundance relative to the Sun, not the ratio of heavy element abundances with respect to each other), the best fit is similar to the bremsstrahlung model but requires a quite low abundance of heavy elements (0.15 solar).

8. THE ORBITAL SOFT X-RAY DIP

The presence of a soft X-ray dip at phase 0.7 is well supported by the *ROSAT* and *EXOSAT* observations. We regard it as a true recurrent feature in the binary.

However, it is definitely transient. It should have been seen by *Einstein* and was not. Was this because of some temporary posteruption effect? Possibly; *ASCA* lacked the low-energy response needed to see the *ROSAT* dip, so we cannot use that result (no dip) to study this question. But since the derived N_{H} in the *ASCA* observation was relatively high, it would not be correct to link declining N_{H} to time since outburst. A more promising possibility is that dip appearances are linked to episodes of low N_{H} , whenever they occur.

As for the cause of the dip, the “standard model” of WZ Sge (Krzemiński & Smak 1971) offers a reasonable explanation. In that model, the mass-transfer bright spot reaches inferior conjunction at orbital phase 0.79 ± 0.02 (corresponding to the preeclipse maximum of the optical photometric wave). At this time it is positioned to obscure the white dwarf and central regions of the disk, if it extends sufficiently high above the disk. The orbital inclination must be $\sim 75^\circ$, in order to eclipse a feature at the disk edge and yet fail to eclipse the white dwarf. So the X-ray-obscuring cloud must extend at least 15° above the disk, and 30° is likely since the dip is fairly long.

U Geminorum must be of similar binary inclination, since it too shows an eclipse of the bright spot but not the white dwarf. This star shows very strong soft X-ray emission in outburst, which arises strictly from the white dwarf/boundary layer, and weak hard X-ray emission in quiescence. The soft X-rays are strongly eclipsed whenever the bright spot transits the line of sight to the white dwarf (Mason et al. 1988; Szkody et al. 1996). Thus it appears to be a good counterpart to WZ Sge.

Is such a feature seen in high-inclination CVs generally? It should be, since all should have mass-transfer bright spots extending presumably as high above the orbital plane as that of WZ Sge. But the X-ray orbital light curves shown by Richman (1996) give only a few weak examples and are basically inconsistent with this expectation. The reason might lie in the speculation offered above, that orbital dips are associated with states of low average N_{H} . In other words, the extra N_{H} associated

with the bright spot is significant only when absorption from other sources (e.g., the flared disk) is low—and the latter condition is hard to achieve when the disk is nearly edge-on. This predicts that in low-energy detectors such as the *Einstein* IPC and the *ROSAT* PSPC, deeply eclipsing CVs⁴ ought to show only a weak and highly absorbed X-ray flux, which arises perhaps from X-rays scattered above the orbital plane. This seems roughly consistent with observation.

9. THE RAPID OSCILLATIONS

9.1. Puzzles and Credentials

The properties of the 28 s oscillations in 1971–1978 were studied by RNP and P80. The former favored interpretation as nonradial pulsations of the white dwarf because of the non-commensurate closely spaced frequencies, and the latter favored interpretation as the signature of a rapidly rotating magnetic white dwarf because of the high phase stability of the dominant signal and the presence of “satellite periods” at frequencies seemingly displaced by integer multiples of the orbital frequency (which suggests a high-energy pulsed searchlight illuminating structures moving prograde in the disk).

Progress has been hampered by the long disappearance of the primary signal. Several of the satellite periods have been observed in the intervening 16 years, but they have been transient and not well observed. However, multicolor observations appear to show colors much bluer than the mean color of the star (Skidmore et al. 1997). The corresponding blackbody temperature ($>70,000$ K) exceeds the temperature of known pulsating hydrogen-rich white dwarfs (the ZZ Ceti stars, with $T_e = 11,000$ – $14,000$ K)—and also far exceeds the temperature of the white dwarf in WZ Sge, known from *HST* data to be 14,800 K (Cheng et al. 1997). This makes it unlikely that the signals are connected with the ordinary white dwarf photosphere and therefore seems to rule out white dwarf pulsation. But the pulsation colors reported by Skidmore et al. are of the satellite signals rather than the primary signal, so this is not quite the right test.

Detection of pulsed X-rays is the *ne plus ultra* test of magnetically channeled accretion. P80 presented the basic argument: the short period and high coherence of the signal demand an origin in the white dwarf, and only channeled radial accretion flow can produce a pulsed signal rich in hard X-rays. The magnetism is not directly observed but is inferred as the only easy way to understand the channeling of the flow. The *ASCA* observation seems to show pulsed X-rays and hence membership in the “DQ Herculis” class of variable stars.

However, this assignment is not beyond question. The *ASCA* detection is weak, and it required significant data massage (soft/hard partition, plus prior knowledge of the period) to uncover. And the “high phase stability” cited above is not exactly right;

⁴ For CVs of sufficiently high \dot{M} . Binaries of very low \dot{M} might give a fairly transparent line of sight to the white dwarf, even at low X-ray energies.

in all years of good coverage (1976, 1978, 1995, and 1996), significant phase wander of ~ 3 s from a best-fit ephemeris occurred on timescales of a few hours.⁵ While we can make excuses for such misadventures (X-ray absorption, presence of unresolved sidebands of rapidly varying amplitude, etc.), they still undermine the security of the argument. So does the very existence of the 29 s clock. We could not find any actual evidence for its interpretation as arising from “disk reprocessing.” There seems to be no numerical relation to P_{orb} , $O - C$ analysis gave no evidence of greater instability (as would be expected since the disk proper cannot support stable structures), and inspection of the power spectrum showed no signal at the 12.2 minute beat period or any extra wandering of the 29 s period. We do not agree with RNP that the 29 s signal is flatly inconsistent with a rotation model of WZ Sge, but we do think that signal is a fact still undigested and unexplained by that model.

9.2. More Puzzles

Still more questions remain. Do we understand why the 27.87 s signal was unobserved for 16 years and then returned? Certainly not. But we do not truly believe it was absent; we suspect that an underlying 27.87 s signal is probably needed to power the sideband signals that were occasionally observed. Typical upper limits from the nondetections were ~ 0.002 mag semiamplitude, and the average semiamplitude in 1995/1996 was 0.003 mag. That difference is too small to rely on as evidence. From study of the preeruption (1970s) signal, we know that large changes in signal amplitude occur over a time-scale as short as a few hours, so the “disappearance” may simply be a combination of a small fading of the signal and a large fading of astronomers’ tenacity.

Do we understand why the signal disappeared in outburst? Yes. A short P_{orb} and low \dot{M} strongly favor spin-orbit synchronism, and to avoid this we must invoke quite a low surface magnetic field for the white dwarf: probably $(1-5) \times 10^4$ G. At this low a field strength, the magnetosphere is squashed down onto the white dwarf during outburst, when the accretion rate jumps by a factor ~ 1000 . Thus the field is too weak to channel accretion flows at high \dot{M} .

Do we understand why the X-ray pulses are so weak? Perhaps. The accretion rate is very low, so the magnetospheric radius is expected to be large. But the white dwarf rotates rapidly, so little of the gas can latch onto field lines as they whirl quickly by. On the contrary, slowly moving gas (in Keplerian orbits just outside the magnetosphere) will be slapped by the rapidly moving field lines and flung farther away. Thus rapid rotation acts as a centrifugal barrier to inhibit accretion

⁵ The reason for claiming (P80) high phase stability in spite of this fact is that the observed degree of scatter over a season (Fig. 5 of P80) is too low to be consistent with a truly poor clock. The 28 s clock of WZ Sge is buffeted severely over a few hours but keeps (or kept in 1978, the only adequately tested year) good time over a few months.

(see, e.g., Wynn, King, & Horn 1997). Some diffusion across field lines can still occur, which produces unpulsed emissions.

There are also geometric ways to obtain weak pulses. If the magnetic pole is close to the rotation pole, then weak pulses are produced as the accreting pole may never disappear over the limb during the spin cycle. And if the true rotation period is 55.74 s, then a small pulsed fraction may occur as one of the accretion columns is visible at all times. Finally, the hard/soft phase shift suggested by Figure 12 may seriously dilute the pulse fraction.

Do we understand why the dwarf nova eruptions are so rare? Yes, probably we do—because of the central cavity carved out by the magnetic field. Accretion disks with central cavities have rather different eruption properties because “inside-out” eruptions cannot occur (Angelini & Verbunt 1989; Livio & Pringle 1992). This means that low \dot{M} alone is enough to yield very long waits between eruptions (Meyer & Meyer Hoffmeister 1994; Lasota, Hameury, & Hure 1995), without requiring very low viscosity (Smak 1993; Osaki 1995; Cannizzo, Shafter, & Wheeling 1988).

10. WEAK MAGNETISM: KEY TO THE WZ SGE CLASS?

The latter point provides a springboard for some vigorous speculation. There are a few stars that show essentially all the normal bona fides of the SU UMa class but show very long intervals between supermaxima and quite rare normal maxima as well (in some cases, perhaps none). These are known as the WZ Sge stars (Bailey 1979; Downes & Margon 1981; O’Donoghue et al. 1991). They are all intrinsically faint, so the long waits between supermaxima are in principle explainable as the result of low \dot{M} . But “inside-out” eruptions should still occur quite frequently, independent of \dot{M} , and this is contradicted by observations of WZ Sge stars. Magnetism appears to give a satisfactory excuse for the prototype, WZ Sge itself. Could this excuse apply to all stars in the (sub)class?

Yes, we think this is possible. The magnetic field required to carve out a central disk cavity, without making the star observably magnetic (an AM Her or DQ Her star), is in the range 10^3-10^5 G. Magnetic fields of this strength could indeed be very common in white dwarfs because detection from Zeeman-split spectral lines becomes difficult for field strengths below 10^5 G. Thus the magnetic hypothesis is plausible and violates no observational constraint. A related possibility is rapid rotation. In the case of zero magnetic field this should not strictly affect the disk (being confined to the disk/star boundary layer), but with a magnetic field present the rapid rotation interposes a significant extra barrier to accretion. In this case we obtain not only a central cavity (suppressing the inside-out eruptions) but also a centrifugal barrier that will inhibit accretion (which renders the star fainter in quiescence, as required by observation). Thus rapid rotation tends to favor systems with the desired characteristics. WZ Sge stars may

possibly be the subclass of low- \dot{M} dwarf novae that have white dwarfs sufficiently magnetic (barely) to dominate accretion flow at quiescence.

11. ULTRAVIOLET SPECTROSCOPY

Cheng et al. (1997) studied the profiles of various low-excitation absorption lines (principally C I) in the ultraviolet spectrum and found that they are best fitted by a white dwarf with $v_{\text{rot}} \sin i = 1200 \pm 300 \text{ km s}^{-1}$. This corresponds to $v_{\text{rot}} = 1240 \pm 300 \text{ km s}^{-1}$, since the grazing-eclipse geometry constrains the inclination fairly well at $i \sim 75^\circ$. For a rotation period of 28 s, this implies a white dwarf radius of $(5.5 \pm 1.3) \times 10^8 \text{ cm}$, which is appropriate for a white dwarf of $0.8\text{--}1.1 M_\odot$.

This provides a strong piece of evidence in favor of the rotation hypothesis for the periodicity. But there are still a few puzzling features that need explanation. One is the issue of the white dwarf mass. Cheng et al. did not agree with the mass range we deduce but instead relied strongly on their best-fitting gravity of $\log g = 8$. With $R = (5.5 \pm 1.3) \times 10^8 \text{ cm}$, the latter formally implies a white dwarf mass $M = 0.23 \pm 0.11 M_\odot$. Cheng et al. favored a comparably low value, but we consider this very unlikely. The Hamada-Salpeter mass-radius relation and $P_{\text{spin}} = 28 \text{ s}$ sets a hard limit of $M > 0.5 M_\odot$ and a still higher practical limit since at this mass the star is entirely supported by rotation and the gravity is negligible! We would reason as follows. The radius deduced from the rotation hypothesis and the Hamada-Salpeter relation together imply $M = 0.8\text{--}1.1 M_\odot$; these masses give breakup spin periods in the range 11–5 s and hence tolerate $P_{\text{spin}} = 28 \text{ s}$ without turning the star into a pancake. This mass range normally leads to $\log g = 8.3\text{--}8.8$, but this would be slightly lower if the star is somewhat oblate. Therefore even a small allowance for uncertainty in $\log g$, or the star’s oblateness, permits masses at least as high as $0.8 M_\odot$, which we consider desirable (actually, mandatory) for the star’s stability.⁶

The ultraviolet power spectrum is also confusing. The strongest signal occurred at 28.20 s on the two occasions at which it was observed, not at 27.87 s as we would have expected (Welsh et al. 1997; C. A. Haswell 1997, private communication). And Welsh et al. (1997) showed a flux spectrum of the pulsed light (at 28.20 s) with possible Ly α absorption, perhaps arising in the white dwarf photosphere. These puzzles do not disturb the line-profile evidence favoring rapid rotation, but

⁶ Cheng et al. quote with approval Smak’s (1993) recent estimate of $M = 0.45 M_\odot$. But, as Smak points out, this estimate depends critically on an uncertain assumption: that the $K_1 = 46 \text{ km s}^{-1}$ term from spectroscopy represents the true dynamical motion of the white dwarf. The K_1 motion in the spectroscopy of Gilliland, Kemper, & Suntzeff (1986) reached maximum recession at orbital phase 0.83 ± 0.01 , whereas the standard model predicts a phase 0.71 ± 0.02 . This discrepancy seems too large to tolerate, and we are inclined to regard 46 km s^{-1} as an upper limit to the true dynamical motion. In effect, this gives a *minimum* white dwarf mass of about $0.45 M_\odot$.

they certainly remind us how little we understand about the period structure!

12. A PULSATION MODEL

The magnetic model discussed above has serious problems. Phase jitter in the pulse timings, the lack of obvious and strong X-ray pulses, and the very existence of the 29 s pulses are all unnatural, hard-to-explain features. A pulsation model, with a nonradially pulsating white dwarf, is also a worthy candidate. In fact, such a star seems to have been discovered in GW Lib, another low- \dot{M} dwarf nova of long recurrence time (B. Warner 1997, private communication). But the signals in GW Lib closely resemble garden-variety white dwarf pulsations: period $\sim 500 \text{ s}$, pulse amplitude $\sim 0.05 \text{ mag}$, multiperiodic structure, and high phase stability. WZ Sge offends the norm in these respects⁷ and is difficult to place under the same rubric. Thus it might be necessary to consider it as the “first WZ Sge star” rather than simply another ZZ Cet star. This makes the pulsation hypothesis disturbingly flexible.

That is really our principal distrust of the pulsation model: it achieves its superiority mainly *by not making any predictions*. The white dwarf merely happens to be pulsating, but the pulsation is not considered as part of the accretion process, so there are no predictions about how any observable properties should be affected by accretion events. A wide range of behavior can be pronounced as acceptable because the cohort of pulsating white dwarfs spans a wide range in power spectrum complexity.

The hypothesis nevertheless remains viable. We favor and extensively discuss a rotation-with-magnetism scenario not so much because of compelling evidence but rather because it is scientifically fruitful, which leads to interesting predictions. The fact that some of these predictions *fail* is quite embarrassing, but it is not quite enough to scare us away from the model. It would be very desirable if pulsation advocates would develop an alternative theory in detail.

13. SUMMARY

1. We report on the return of the 27.87 s signal in 1995–1996 optical photometry of WZ Sge. The properties of the oscillation were roughly as they were observed during 1976–1978. The mean semiamplitude was 0.003 mag. The main power spectrum peaks occurred at the same periods seen previously, mainly 27.87 and 28.96 s, but an extra signal was also seen at 29.69 s. The signals are obviously noncommensurate and do not occur

⁷ Although we have described WZ Sge as generally multiperiodic and stable in phase, we would not do so in the context of comparison with known ZZ Cet stars. The latter often have dozens or hundreds of separate frequencies (rather than two or three) and show amplitude and phase changes that are believed to be the result of the beating of these many signals rather than signifying a truly unstable clock. The 27.87 s signal in WZ Sge was measured fairly well in 1978 when other signals were very weak, and the phase did wander erratically by $\sim 3 \text{ s}$ on a timescale of just a few hours.

at orbital sidebands. We could not discover whether they are truly independent in their physical origin.

2. Amplitude changes were sufficiently great that we could not establish a unique cycle count for the shorter period signal. The best period from observations on individual nights in 1995/1996 was 27.877 ± 0.010 s. On the assumption that phase coherence is in fact present, the precise period in 1996 was 27.8757 or 27.8666 (± 0.0001) s. For the longer period signal, we obtained one episode of dense coverage which suggested a precise period of 28.9593 ± 0.0005 s. However, we regard the five night basis for this measurement as too small to really prove an underlying high stability.

3. The ASCA X-ray observation yielded a significant detection of the 27.87 s signal in the 2–6 keV energy band. This favors identification of WZ Sge as a DQ Her star, in which a magnetic field channels accretion onto the rapidly spinning white dwarf.

4. The hard X-ray and soft X-ray light curves on the likely 27.87 s spin period appear to be out of phase by $\sim 180^\circ$. This may arise because the soft X-rays reach minimum at the “pole-on” position, where the accretion column presents maximum opacity to X-rays emitted in our direction.

5. It is possible that the “satellite periods” seen in the low-frequency wing of the 27.87 s signal arise from reprocessing in structures moving prograde in the disk. But the 28.96 s signal is extremely vexing. Blobs orbiting with $P = 12.2$ minutes could make such a signal, but this produces multiple puzzles because it is incommensurate with P_{orb} , does not leave any independent signature in the data, and is hard to reconcile with high phase stability (because such a feature tends to be destroyed by the highly sheared flow in the disk). Most of these difficulties also apply to the 29.69 s. These issues are important to resolve if we are to really believe in the rotation model.

6. We also briefly discuss the pulsation model. In this model the white dwarf merely happens to be pulsating, not as a result of accretion. Pulsation naturally accounts for noncommensurate periods but fails to explain the pulsed X-rays or the orbital sidebands.

7. A short P_{orb} and low \dot{M} strongly favors spin-orbit synchronism, and to avoid this we must invoke quite a low surface magnetic field for the white dwarf: probably $(1-5) \times 10^4$ G.

8. The ROSAT observation showed a distinct orbital modulation in soft X-rays, with maximum soft X-ray absorption near orbital phase 0.7. This roughly corresponds to inferior conjunction of the mass-transfer bright spot in the “standard model” for WZ Sge, so it is reasonably explained as obscuration of the central X-ray source by a vertically puffed-up structure at the bright spot. In order to produce a wide ($0.2P_{\text{orb}}$) dip, that structure must also be quite extended in azimuth. But the optical eclipse of the bright spot reveals quite a small object ($R \sim 10^9$ cm), which must be just the central core of the bright spot.

9. It has proved difficult to understand the WZ Sge stars, the dwarf novae of longest recurrence time. Since the prototype star may well contain a rapidly rotating magnetic white dwarf, one wonders if that can explain the observed behavior in the class. A weak magnetic field can indeed allow the required very long outburst times by carving out a central cavity in the disk. Rapid rotation seems less critical, although it can play a role by interposing a centrifugal barrier to accretion in quiescence. The required signature would be a stable short period in the light curve, and searches for these signals are warmly recommended.

This research was supported in part by NASA grant NAG5-4734 and NSF grant AST96-18545.

REFERENCES

- Angelini, L., & Verbunt, F. 1989, MNRAS, 238, 697
 Bailey, J. A. 1979, MNRAS, 189, 41P
 Cannizzo, J. K., Shafter, A. W., & Wheeler, C. 1988, ApJ, 333, 227
 Cheng, F., Sion, E. M., Szkody, P., & Huang, M. 1997, ApJ, 484, L149
 de Korte, P. A. J., et al. 1981, Space Sci. Rev., 30, 495
 Downes, R. A., & Margon, B. 1981, MNRAS, 197, 35P
 Eracleous, M. H., Halpern, J. P., & Patterson, J. 1991a, ApJ, 382, 290
 Eracleous, M. H., Patterson, J., & Halpern, J. P. 1991b, ApJ, 370, 330
 Giacconi, R., et al. 1979, ApJ, 230, 540
 Gilliland, R., Kemper, E., & Suntzeff, N. 1986, ApJ, 301, 252
 Groth, E. 1975, ApJS, 29, 825
 Krzemiński, W., & Kraft, R. P. 1964, ApJ, 140, 921
 Krzemiński, W., & Smak, J. 1971, Acta Astron., 21, 133
 Lasota, J. P., Hameury, J. M., & Hure, J. M. 1995, A&A, 302, L29
 Livio, M., & Pringle, J. E. 1992, MNRAS, 259, 23P
 Long, K. S., Mauche, C. W., Raymond, J. C., Szkody, P., & Mattei, J. A. 1996, ApJ, 469, 841
 Mason, K. O., Córdova, F. A., Watson, M. G., & King, A. R. 1988, MNRAS, 232, 779
 Meyer, F., & Meyer Hoffmeister, F. 1994, A&A, 288, 175
 Middleditch, J., & Nelson, J. E. 1980, BAAS, 11, 664
 O’Donoghue, D., Chen, A., Marang, F., Mittaz, J. P. D., Winkler, H., & Warner, B. 1991, MNRAS, 250, 363
 Osaki, Y. 1995, PASJ, 47, 47
 Patterson, J. 1980, ApJ, 241, 235 (P80)
 Patterson, J., McGraw, J. T., Coleman, L. A., & Africano, J. L. 1981, ApJ, 248, 1067
 Richman, H. R. 1996, ApJ, 462, 404
 Robinson, E. L., Nather, R. E., & Patterson, J. 1978, ApJ, 219, 168 (RNP)
 Sion, E. M., Cheng, F. H., Long, K. S., Szkody, P., Gilliland, R. L., Huang, M., & Hubeny, I. 1995, ApJ, 439, 962
 Skidmore, W., Welsh, W. F., Wood, J. H., & Steining, R. F. 1997, MNRAS, 288, 189
 Smak, J. 1993, Acta Astron., 43, 101
 Szkody, P., Long, K. S., Sion, E. M., & Raymond, J. C. 1996, ApJ, 469, 834
 Welsh, W. F., et al. 1997, MNRAS, in press
 Wynn, G. A., King, A. R., & Horne, K. 1997, MNRAS, 286, 436